Comparison of Eye Morphology and Retinal Topography in Two Species of New World Vultures (Aves: Cathartidae)

THOMAS J. LISNEY,[1]* KARYN STECYK,[1] JEFFREY KOLOMINSKY,[2]
GARY R. GRAVES,[3,4] DOUGLAS R. WYLIE,[1,2] AND ANDREW N. IWANIUK[5]
[1]Department of Psychology, University of Alberta, Edmonton, AB, Canada
[2]Center for Neuroscience, University of Alberta, Edmonton, AB, Canada
[3]Division of Birds, National Museum of Natural History, Smithsonian Institution,
Washington, DC
[4]Center for Macroecology, Evolution and Climate, University of Copenhagen, DK-2100,
Copenhagen Ø, Denmark
[5]Department of Neuroscience, Canadian Center for Behavioral Neuroscience, University of
Lethbridge, Lethbridge, AB, Canada

ABSTRACT

Vultures are highly reliant on their sensory systems for the rapid detection and localization of carrion before other scavengers can exploit the resource. In this study, we compared eye morphology and retinal topography in two species of New World vultures (Cathartidae), turkey vultures (*Cathartes aura*), with a highly developed olfactory sense, and black vultures (*Coragyps atratus*), with a less developed sense of olfaction. We found that eye size relative to body mass was the same in both species, but that black vultures have larger corneas relative to eye size than turkey vultures. However, the overall retinal topography, the total number of cells in the retinal ganglion cell layer, peak and average cell densities, cell soma area frequency distributions, and the theoretical peak anatomical spatial resolving power were the same in both species. This suggests that the visual systems of these two species are similar and that vision plays an equally important role in the biology of both species, despite the apparently greater reliance on olfaction for finding carrion in turkey vultures. Anat Rec, 296:1954–1970, 2013.   © 2013 Wiley Periodicals, Inc.

Key words: bird; *Cathartes aura*; *Coragyps atratus*; olfaction; retinal ganglion cell; scavenging; sensory ecology; vision; visual acuity

Vultures are important for healthy ecosystem functioning because they recycle carcasses and lead other scavengers to carcasses, facilitating the flow of energy and nutrients through food webs and reducing the risk of infectious disease (DeVault et al., 2003; Sekercioglu 2006; Wilson and Wolkovich, 2011). Vultures face heavy competition for carrion from other avian scavengers, a host of small to medium-sized mammals (Wallace and Temple, 1987a; Prior and Weatherhead, 1991; Buckley, 1996; Smith et al., 2002; DeVault et al., 2011), and insects and microbes, which can rapidly render a carcass unpalatable (DeVault et al., 2003; Beasley et al., 2012).

Because vultures are almost entirely dependent on carrion, they rely heavily on their sensory systems, in particular vision (Martin et al., 2012; Spiegel et al., 2013), to rapidly detect and locate carcasses before other scavengers arrive and exploit the resource (DeVault et al., 2003; Rajchard, 2008). However, when foraging, vultures are not able to see directly forward (Martin et al., 2012). This makes them highly vulnerable to collisions with anthropogenic structures such as power lines and wind turbines, and also aircraft. Such collisions can be a significant cause of mortality, large enough to cause significant population declines, and are cause of growing concern (Martin, 2011; Martin et al., 2012).

Unusually among vultures, three species of New World vulture (Cathartidae), of the genus *Cathartes*, are thought to primarily rely on olfaction to detect and locate carcasses, whereas the remaining four species in the family appear to rely primarily on vision (Stager, 1964; Houston, 1984, 1986; Graves, 1992; Gomez et al., 1994; Buckley, 1996). Particular attention has been paid to the roles of olfaction and vision in the foraging behavior of turkey vultures (*Cathartes aura*) and black vultures (*Coragyps atratus*), the two most common and widely distributed cathartid species (Bang, 1964; del Hoyo et al., 1994; Ferguson-Lees and Christie, 2001). Behavioral studies and observations have shown that turkey vultures are able to detect carrion in the absence of visual cues (Stager, 1964; Houston, 1986, 1988; Buckley, 1996). Moreover, although rigorously quantified data on foraging height are lacking, turkey vultures tend to forage relatively close to the ground where odors are concentrated and this species generally arrives at carcasses before other scavengers (Houston, 1986, 1988; Wallace and Temple, 1987a; Buckley, 1996; Stolen, 2000; Smith et al., 2002). In contrast, black vultures forage at higher altitudes, thereby allowing them to scan larger areas for potential food sources and also to spot cathartid vultures, which they often follow to a carcass (Houston, 1986, 1988; del Hoyo et al., 1994; Buckley, 1996; Stolen, 2000; Smith et al., 2002; Walter et al., 2012). Furthermore, the olfactory system differs between these two species; turkey vultures have larger nostrils (Fig. 1), a larger nasal fossa, a greater surface area for olfactory receptors, and relatively larger olfactory bulbs than black vultures (Bang, 1964; Stager, 1964; Bang and Cobb, 1968).

In contrast to olfaction, very little is known about vision in cathartid vultures. Some information on retinal organization is available for three species, turkey and black vultures and Andean condors (*Vultur gryphus*) (Lord, 1956; Inzunza et al., 1989, 1991), but a detailed, direct comparison of the visual system of the *Cathartes* species with acute olfactory abilities and that of the other New World vultures that are believed to rely primarily on vision is lacking. The aim of this study was to directly compare the visual systems of turkey vultures and black vultures (Fig. 1), concentrating on eye morphology and the topography of the retinal ganglion cell (RGC) layer. Eye size and morphology are useful indicators of the relative importance of vision and are correlated with feeding behavior in birds (Ritland, 1982; Brooke et al., 1999; Garamszegi et al., 2002; Howland et al., 2004). RGCs are the only source output of the retina (Hughes, 1977; Pettigrew et al., 1988) and mapping the topographic distribution of the RGCs permits the identification of retinal specializations (i.e., areae,
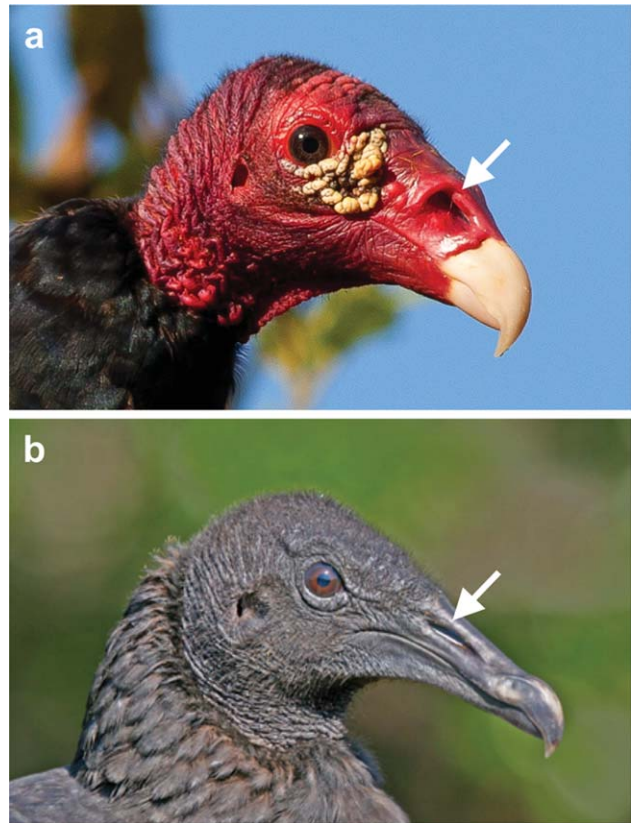

Fig. 1. Photographs of a turkey vulture (*Cathartes aura)* (**a**) and a black vulture (*Coragyps atratus*) (**b**). Both species have prominent, laterally placed eyes, which appear to be similarly sized and positioned. Also note the large size of the nostrils (arrowed) in the turkey vulture compared to the black vulture. Turkey and black vulture photographs are courtesy of, and reproduced with permission from Brian Schmidt, Washington DC, USA and Bryan Jones, Utah, USA, respectively.

foveae, and visual streaks) that are closely associated with behavioral ecology and feeding behavior in birds (Meyer, 1977; Moroney and Pettigrew, 1987; Hayes and Brooke, 1990; Inzunza et al., 1991; Boire et al., 2001; Coimbra et al., 2006, 2009, 2012; Dolan and Fernández-Juricic 2010; Lisney et al., 2012a,b). Moreover, a combination of the posterior nodal distance (PND) of the eye (the distance from the posterior nodal point of the eye to the choroid-retina boundary) and RGC spacing can be used to calculate the theoretical upper limit of spatial resolving power (SRP) (Ullmann et al., 2012), a measure of the eyes ability to discriminate fine detail, thus allowing visual acuity to be compared among species (Moroney and Pettigrew, 1987; Wathey and Pettigrew, 1989; Dolan and Fernández-Juricic, 2010; Coimbra et al., 2012; Lisney et al., 2012b; 2013).

Because turkey vultures are considered to be olfactory specialists, we predicted that the visual system of this species could have undergone a reduction compared to that of black vultures. Sensory systems are metabolically expensive (Laughlin, 2001a,b; Niven and Laughlin, 2008) and so specialization in one sensory modality can result in an evolutionary trade-off whereby other sensory modalities become regressed (Stevens, 2013). Such trade-offs have been illustrated in a variety of animals

by comparing the size and morphological configuration of different sense organs and/or the number of sensory receptor cells associated with different modalities among species (e.g., Livingston, 1987; Pettigrew et al., 1998; Martin et al., 2007; Martin and Piersma, 2008; Gunter and Meyer, 2013). Given the difference in the use of olfactory versus visual cues between turkey and black vultures, we therefore predicted that turkey vultures would have relatively smaller eyes, fewer cells in the RGC layer, and lower SRP than black vultures. Surprisingly, we found that eye size relative to body mass, retinal topography and SRP were very similar in turkey and black vultures, although differences in the shape of their eyes were significant.

MATERIALS AND METHODS

Animals

Turkey vultures and black vultures were collected in the vicinity of Nashville, Tennessee, USA by the United States Department of Agriculture (USDA) Animal and Plant Health Inspection (APHIS) Wildlife Services in February 2012. Vultures were collected by the USDA APHIS Wildlife Services (Nashville) under US Fish and Wildlife Service permit #MB018937-0. Before the eyes were removed from the head, each bird was weighed (g) and the limbus of each eye was marked dorsally and nasally, allowing the eyes and retinas to be orientated after excision. Eyes were removed and immersion fixed in 4% buffered (pH = 7.4) paraformaldehyde, and then left in fixative for several weeks prior to further processing. Voucher specimens are deposited in the research collections of the Division of Birds, National Museum of Natural History, Smithsonian Institution, Washington, DC, USA.

Eye Morphology

Linear measurements were made for 16 eyes (eight eyes from eight individuals of each species). Each eye was cleaned of all fascia and extraocular muscles and then the transverse diameters of the eye and the cornea were measured along two perpendicular planes using digital callipers, as described in Lisney et al. (2012b) (Fig. 2). This gave a maximum and a minimum measurement for both transverse eye diameter and corneal diameter. These measurements were then used to calculate mean corneal diameter (C), mean transverse eye diameter (T), and the ratio of the two, that is the $C{:}T$ ratio (Kirk, 2004, 2006a,b), which we used as a measure of eye shape (following Hall and Ross, 2007). Eyes were also "reinflated" with fixative using a syringe and a small-gauge needle (Kirk, 2004, 2006a,b; Hall and Ross, 2007; Lisney et al., 2012a,b, 2013). We then measured the transverse diameters of the eye and the cornea again for the six turkey vulture and five black vulture eyes that could be reinflated. This allowed us to confirm that there were no significant differences between $C{:}T$ calculated from corneal and eye diameter measurements made before and after reinflation (paired t test on pooled $\log_{10}$ transformed data; t = 1.80, df = 10, P = 0.10). Replication of measurements showed a high degree of repeatability (r = 0.98; Lessells and Boag, 1987). Because we found no significant difference in $C{:}T$ between inflated and uninflated eyes, and in order to maximize our sample size, we used the measurements made from uninflated eyes to calculate $C{:}T$, as we have done in previous studies (Lisney et al., 2012b, 2013).

Axial length (A) of the eye (the distance from the anterior portion of the cornea to the most posterior part of the sclera) was also measured for the eyes that could be reinflated (Hall and Ross, 2007; Iwaniuk et al., 2010; Lisney et al., 2012a,b, 2013). A was used to calculate $C{:}A$, the ratio of mean corneal diameter to axial length (Kirk, 2006a; Hall and Ross, 2007; Veilleux and Lewis, 2011; Lisney et al., 2012a,b, 2013). Both $C{:}T$ and $C{:}A$ provide a measure of cornea size relative to the total size of the eye (Kirk, 2006a). The two ratios in turkey and black vultures (pooled) were significantly correlated with one another (Pearson r = 0.91, df = 8, P = 0.0003).
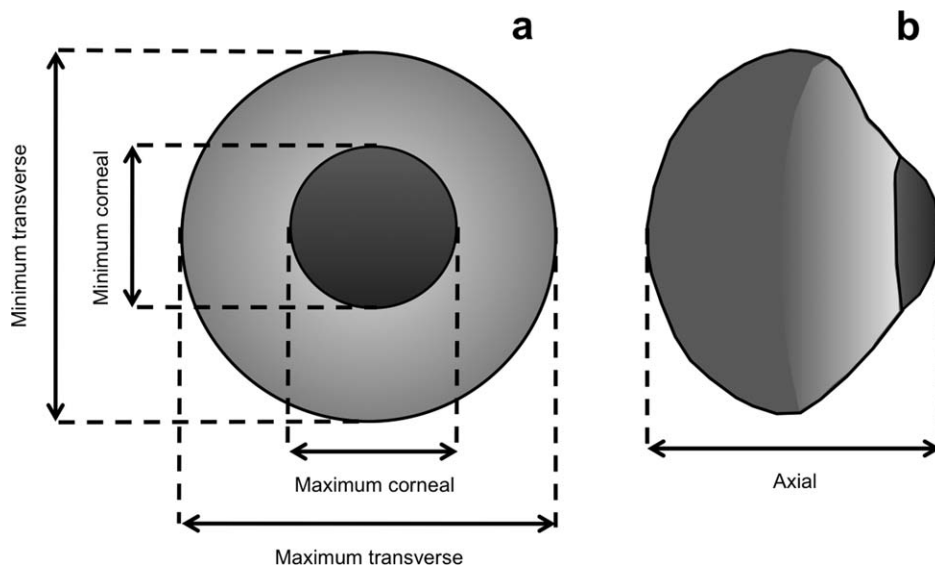

Fig. 2. Diagrams showing dorsal (**a**) and lateral (**b**) views of a turkey vulture eye. The diagrams illustrate the measurements of (a) corneal and eye transverse diameter, and (b) eye axial length.

Ratios of T and A to body mass were also calculated in order to assess relative eye size in the two species.

Retinal Whole Mounts

Three retinas for each species were successfully whole mounted, using previously described methods (Stone, 1981; Lisney et al., 2012a,b, 2013; Ullmann et al., 2012). The retinal pigment epithelium was bleached using hydrogen peroxide and the whole mounts were stained for Nissl substance using 0.1% Cresyl Violet (pH = 4.3) (Stone, 1981; Ullmann et al., 2012; Lisney et al., 2012a,b, 2013). We quantified whole mount shrinkage resulting from the staining process by measuring the outline of each whole mount pre- and post-staining from scaled digital photographs, using the public domain NIH image program ImageJ (Rasband 1997–2012). Shrinkage ranged from 1.0–5.5% and was confined to the margins of the whole mount and along the edges of the radial relieving cuts or tears (Stone, 1981; Ullman et al., 2012).

Cell Counts and Estimates of Total Cell Number

Prior to making counts of Nissl-stained cells in the RGC layer, the entire surface of each whole mount was observed using a compound microscope (Leitz Labourlux S) and low power (10× and 20×) objectives. This allowed us to visually inspect each retina and to search for the presence a fovea or foveae (Ullmann et al., 2012). In a whole mount, a fovea can be identified in the RGC layer as a small, circular pit (Bravo and Pettigrew, 1981; Lisney et al., 2012a; Moore et al., 2012). Counts of Nissl-stained cells (Fig. 3) were made using the optical fractionator method (West et al., 1991) modified for the analysis of retinal whole mounts (Coimbra et al., 2009, 2012; Hart et al., 2012; Lisney et al., 2012a,b, 2013). Using a systematic random sampling protocol, digital photo-micrographs of the RGC layer were taken at regular intervals according to defined sampling grids (see below) across each whole mount using a Leitz Labourlux S compound microscope with a 100× oil immersion objective (NA = 1.25), equipped with a IMC-4050FT camera (Imi Tech, Encinitas, CA), a MS-2000 XYZ automated stage and control unit (Applied Scientific Instrumentation, Eugene, OR), and Stereologer software (Stereology Resource Center, www.disector.com). Initially, for one whole mount for each species, we used a sampling grid measuring 1×1 mm^2. This sampling strategy resulted in 553 and 492 points being sampled for the turkey vulture and black vulture whole mounts, respectively. The resultant coefficients of error (CE), calculated using Schaeffer's estimator for a one-stage systematic sample (Schaeffer et al., 1996) for nonhomogeneous distributions (Schmitz and Hof, 2000), were very low (0.023 and 0.018). The CE serves as a measure of the accuracy of a population estimate determined using a stereological sampling procedure, with $CE \leq 0.1$ considered highly reliable (Boire et al., 2001; Coimbra et al., 2009, 2012; Ullmann et al., 2012). In this study, we found that the use of coarser sampling grids still resulted in very low CE values. For the remaining four whole mounts, we used 1.3×1.3 or 1.5×1.5 mm^2 sampling grids, which sampled about 220–330 points per retina and resulted in CE values ≤ 0.03. Where a fovea was identified, its position was also marked on the sampling grid, allowing its

location to be marked accurately on the resultant retinal topography map (see below).

To count cells, an unbiased counting frame (35×35 μm^2) was placed on the center of each digital photomicrograph using ImageJ. We counted Nissl-stained cells if they lay entirely within the counting frame or if they touched an acceptance line without also touching a rejection line (Gundersen, 1977). Glial cells, which were identified on the basis of their small size, elongate spindle or cigar-like shape and dark staining (Hughes, 1985; Wathey and Pettigrew, 1989; Coimbra et al., 2009), were not included in the counts. We did not differentiate between RGCs and displaced amacrine cells also found in the RGC layer because we could not reliably distinguish between the two cell types using cytological criteria in the areas of high cell density (Lisney et al., 2012a,b, 2013).

When using the optical fractionator modified for retinal whole mounts, the section sampling fraction (ssf) and thickness sampling fraction (tsf) are both set to 1 (Coimbra et al., 2009, 2012; Hart et al., 2012). This is because the whole mount is considered to be a single section (hence ssf = 1), and the height of the optical dissector is considered to be the same as the thickness as of the RGC layer at all locations across the whole mount, resulting in tsf = 1. Therefore, to determine the total number of cells in the RGC layer for each whole mount, we multiplied the sum of the total number of cells counted by the inverse of the area sampling fraction (asf) (Coimbra et al., 2009, 2012; Hart et al., 2012; Lisney et al., 2012a,b, 2013), which is the area of the counting frame divided by the area of the sampling grid. For example, for a 35×35 μm^2 counting frame and a 1×1 mm^2 sampling grid, the asf = 0.001225 mm^2. As mentioned above, CE values were calculated in order to assess the accuracy of our estimates of total cell number. The CE values were very low for all of our whole mounts (≤ 0.03; Table 2), indicating that our estimates of total cell number were relatively robust.

Maps of Retinal Topography

Cell counts for each counting frame were converted to cell densities (cells mm^{-2}). These data were then used to create isodensity contour plots using DeltaGraph 6 (Red Rock Software, Salt Lake City, UT) (Ahnelt et al., 2006; Schiviz et al., 2008; Lisney et al., 2012b, 2013). The scaled, correctly oriented post-stain outline of each whole mount, traced from a digital photograph (see above), was then superimposed on top of the contour plot in order to complete the topographic map.

Cell Soma Area

Whole mounts were divided into three regions on the basis of cell density and location: (1) "low" density ($<10,000$ cells mm^{-2}) in the retinal periphery, (2) "medium" density (10,000–14,999 cells mm^{-2}) in the visual streak, and (3) "high" density ($\geq 15,000$ cells mm^{-2}) in the central retina (Fig. 3). We then used ImageJ to make two-dimensional areal measures of soma area for 200 cells from randomly selected digital photomicrographs from each region.

Spatial Resolving Power

We estimated the theoretical, peak anatomical spatial resolving power (SRP; expressed in cycles/deg) of the two vulture species using peak cell densities and an
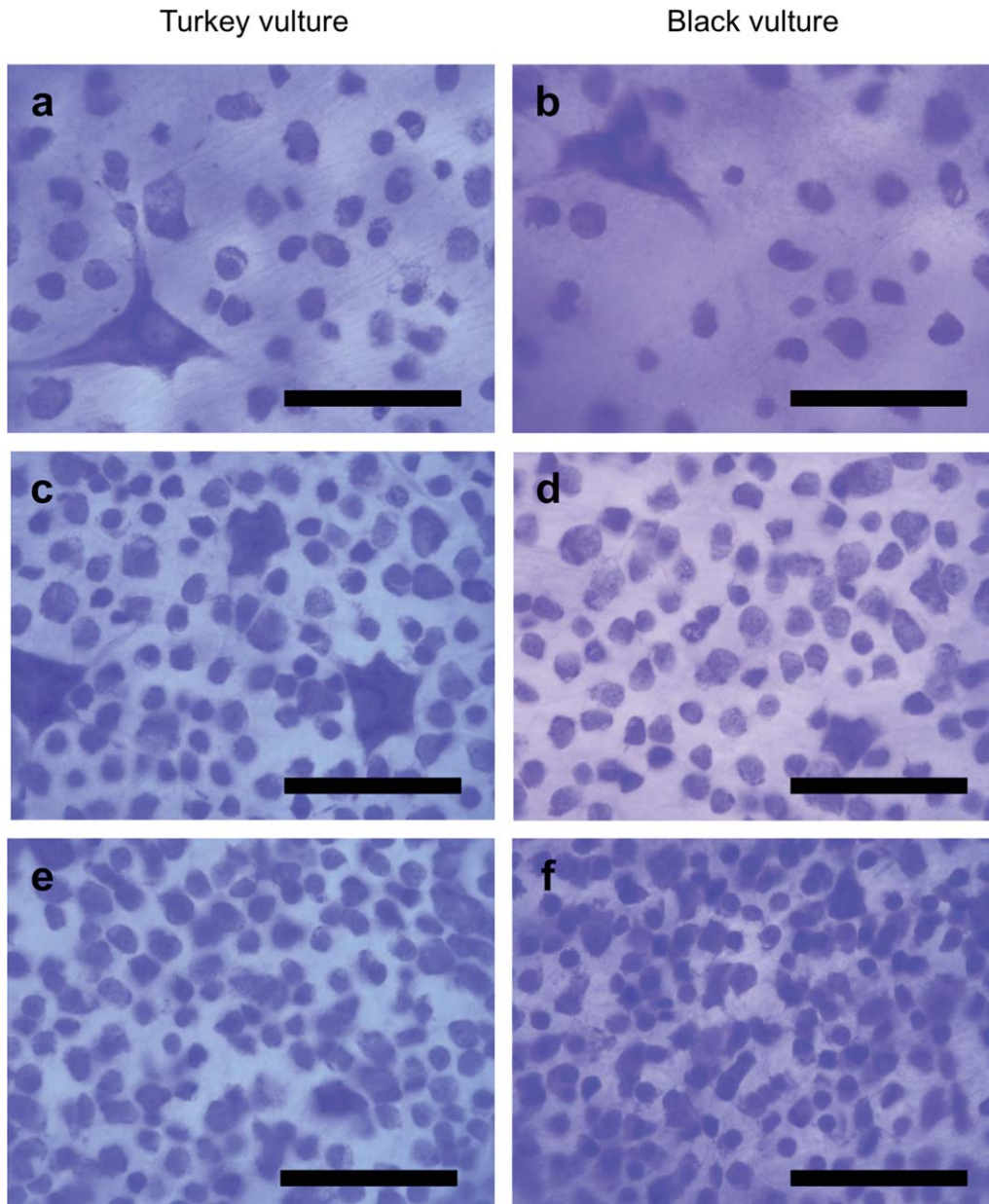
Turkey vulture

Black vulture

Fig. 3. High magnification digital photo-micrographs showing Nissl-stained cells in the retinal ganglion cell (RGC) layer in a turkey vulture (**a**, **c**, **e**) and a black vulture (**b**, **d**, **f**). a and b show cells at low densities ($<$10,000 cells mm^{-2}) in the retinal periphery, c and d show cells at medium densities (10,000–14,999 cells mm^{-2}) in the visual streak and e and f show cells at high densities ($\geq$15,000 cells mm^{-2}) in the central retina, close to the central fovea. Scale bars represent 40 μm. Examples of large cells with prominent dendrites can be seen in a, b and c. These cells were sparsely distributed and were encountered in the low density, and to a lesser extent, medium density regions of the retina in both species.

estimate of the focal length of each eye, following the approach of Hart (2002). PND was used as a proxy for focal length (Hart, 2002; Lisney and Collin, 2008; Lisney et al., 2012b, 2013; Ullmann et al., 2012). The PND was assumed to be 0.6$\times$ of the eye axial length (Hughes, 1977; Martin, 1994; Ullmann et al., 2012).

Statistics

Statistical analyses were performed using Prism 5 (GraphPad Software, San Diego, CA). For interspecific comparisons of eye size and shape, eye size relative to body mass, whole mount area, total cell number, peak and average cell density, cell density gradients and peak SRP, all data were log$_{10}$ transformed and analyzed using unpaired t tests. To analyze cell soma area frequency distributions we grouped the cells we measured into three size categories (0–49 μm^2, 50–99 μm^2, and $\geq$100 μm^2) and assessed the number of cells in each of the three size classes in the low, medium, and high density retinal regions for both species using chi-squared tests. We also analyzed median cell soma area in each of the

three retinal regions using nonparametric statistics. This was done because the frequency distributions of soma area were heavily positively skewed and homogeneity of variances could not be obtained through data transformation.

RESULTS

Eye Morphology

There were no noticeable external differences in eye size between turkey vultures and black vultures (Fig. 1). However, an analysis of eye size measurements (Table 1, Fig. 4) revealed that turkey vulture eyes were significantly larger than those of black vultures in terms of mean transverse eye diameter (T) (t = 4.91, df = 14, $P = 0.0002$), but not eye axial length (A) (t = 2.06, df = 9, $P = 0.07$) (Fig. 4c,d). Body mass was similar (Table 1) and not significantly different (t = 0.74, df = 14, $P = 0.47$) between the two species. Thus, there were no significant differences in either the ratio of T to body mass (t = 1.99, df = 14, $P = 0.0661$), or A to body mass (t = 1.22, df = 9, $P = 0.2527$) (Fig. 4e,f).

Turkey vultures had noticeably smaller corneas relative to eye size (Fig. 4a,b). This difference in eye shape was confirmed by comparing the $C:T$ and $C:A$ values of turkey and black vultures (Table 1; Fig. 4g,h). There were significant differences between turkey and black vultures in both $C:T$ (t = 4.12, df = 14, $P = 0.001$) and $C:A$ values (t = 3.92, df = 9, $P = 0.004$).

Stereology of the RGC Layer

A summary of our stereological sampling of the RGC layer in the two vulture species is provided in Table 2. The average area of the turkey vulture whole mounts (594.0 ± 14.5 mm^2) was significantly larger than that of the black vulture whole mounts 561.4 ± 19.3 mm^2) (t = 2.97, df = 4, $P = 0.04$), which corroborated our analysis of T (see above). The total number of Nissl-stained cells in the RGC layer estimated using our stereological methods averaged $\sim$3.9 million in the turkey vultures and $\sim$3.8 million in the black vultures. Despite the difference in whole mount area between the two species, there was no significant difference in the total number of cells between them (t = 0.65, df = 4, $P = 0.55$). Post-staining retinal whole mount area and total cell number were used to calculate average cell density for each

species (Table 2), which was not significantly different (t = 0.70, df = 4, $P = 0.52$).

Retinal Cell Densities

The distribution of Nissl-stained cells in the RGC layer was similar in both turkey vultures and black vultures (Fig. 5, Table 3). In both species, the lowest cell densities, in the range of 2,040–2,100 cells mm^{-2}, were found in the dorsal and ventral peripheries of the retina. More centrally, a weak visual streak was evident, containing cell densities $\geq$10,000 cells mm^{-2}. The visual streak extended from a point approximately midway between the nasal edge of the retina and the superior pole of the pecten, to a point about midway between the superior pole of the pecten and the temporal edge. Within the visual streak, an area of high cell density containing a fovea was located in the central retina just anterior to the superior pole of the pecten. The peak cell density values (ca., 21,000–24,000 cells mm^{-2}) for all whole mounts were found in this part of the retina. Temporal to this foveate, high density area, a second area of high cell density was present in each of the whole mounts. We did not detect a fovea associated with this temporal high density area. The average cell density gradients for the two species were similar (11.5:1–12:1) and not significantly different (t = 1.01, df = 4, $P = 0.37$). There were no significant differences in the lowest cell density values between the two species (t = 0.77, df = 4, $P = 0.48$), or for either of the two high density areas (central, foveate area: t = 0.95, df = 4, $P = 0.40$; temporal, afoveate area: t = 1.33, df = 4, $P = 0.25$).

Cell Soma Area

Cell soma areas of the turkey and black vulture whole mounts were compared for three retinal regions (Table 4, Figs. 3 and 6). In both species, cell soma area ranged from $\sim$10 to >300 μm^2. In all three retinal regions in both species, the soma area frequency distributions were predominantly unimodal and positively skewed. However, there were differences in frequency distributions among the three retinal regions in both species. On average across both species, in the low density, peripheral regions of each whole mount the majority of cells (63.5%) had soma areas smaller than 49 μm^2 while only 13.3% of the cells had cell soma areas $\geq$100 μm^2. In contrast, in the high density regions of the central retina, cell soma area was relatively more homogeneous, with an average of 94% of the cells having a soma area less

TABLE 1. Body mass, eye size and eye shape in turkey vultures and black vultures

	Turkey vulture; *Cathartes aura*	Black vulture; *Coragyps atratus*
Body mass (kg)	2.11 ± 0.11; ($n = 8$)	2.15 ± 0.09; ($n = 8$)
Mean eye transverse diameter (T) (mm)	22.46 ± 0.24; ($n = 8$)	21.74 ± 0.33; ($n = 8$)
Eye axial length (A) (mm)	18.66 ± 0.03; ($n = 6$)	18.07 ± 0.02; ($n = 5$)
T:body mass ratio	10.67 ± 0.54; ($n = 8$)	10.15 ± 0.48; ($n = 8$)
A:body mass ratio	8.80 ± 0.58; ($n = 6$)	8.43 ± 0.35; ($n = 5$)
Mean corneal diameter (C) (mm)	9.02 ± 0.47; ($n = 8$)	9.72 ± 0.36; ($n = 8$)
$C:T$ ratio	0.40 ± 0.02; ($n = 8$)	0.45 ± 0.02; ($n = 8$)
$C:A$ ratio	0.50 ± 0.03; ($n = 6$)	0.55 ± 0.02; ($n = 5$)

Average values $\pm$SD are presented. The number of birds/eyes assessed for each species (n) is given in parentheses.
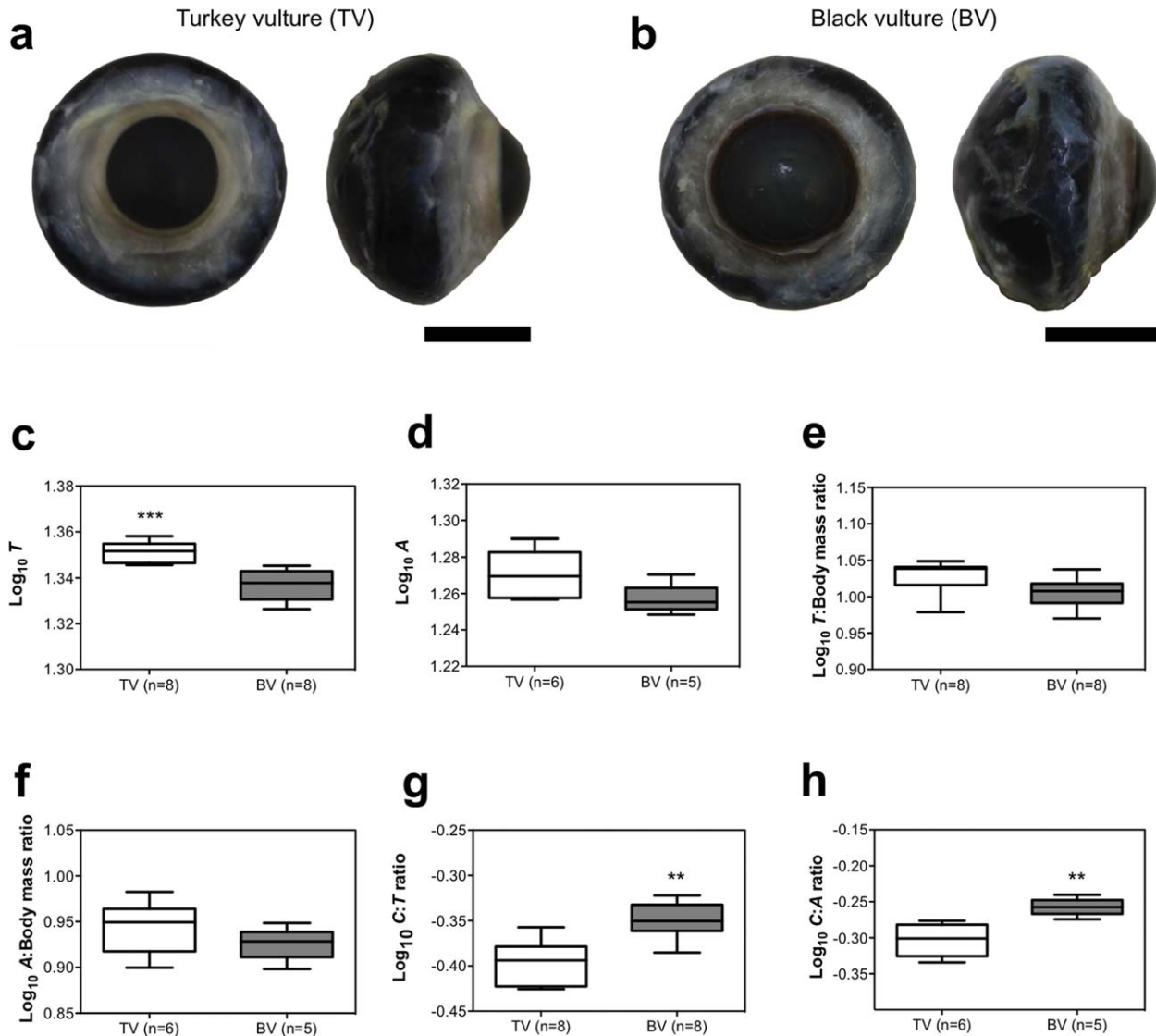
Fig. 4. Eye morphology in turkey vultures and black vultures (abbreviated to TV and BV, respectively). (**a–b**) Dorsal and lateral views of an excised eye from a turkey vulture (a) and a black vulture (b). The scale bars represent 10 mm. (**c–d**) Box-and-whisker plots showing eye size, expressed as (c) mean transverse eye diameter (T) and (d) axial eye diameter (A). (**e–f**) Box-and-whisker plots showing relative eye size expressed (e) using the ratio of mean transverse eye diameter (T) to body mass and (f) the ratio of mean axial eye diameter (A) to body mass. (**g–h**) Box-and-whisker plots showing eye shape, expressed (g) using the ratio of mean corneal diameter to mean transverse eye diameter (C:T) and (h) the ratio of mean corneal diameter to axial eye diameter (C:A). In all of the plots the turkey vulture data are shown in white and the black vulture data are shown in grey. The asterisks in c, g and h indicate significant differences between turkey and black vultures where $P < 0.01$ (**) or < 0.001 (***).

than 49 μm^2 and fewer than 1% of the cells having soma areas $\geq$100 μm^2. In the medium density regions, encompassing the visual streak, an average of 76.7% of the cells had soma areas less than 49 μm^2, with 3.4% of the cells having soma areas $\geq$100 μm^2. Differences in the frequencies of cells within each of the three size categories in each of the three retinal regions were significant in both turkey vultures ($\chi^2 = 70.6$, df $= 4$, $P < 0.0001$) and black vultures (($\chi^2 = 60.1$, df $= 4$, $P < 0.0001$). However, for all three retinal regions, there were no significant differences in the frequencies of cells within each of the three size categories between the two species (low density region: $\chi^2 = 1.71$, df $= 2$, $P = 0.43$; medium density region: $\chi^2 = 1.38$, df $= 2$, $P = 0.5$; high density region: $\chi^2 = 0.52$, df $= 2$, $P = 0.77$).

Additional comparisons of cell soma area between the two species were made by comparing the median soma area among the three retinal regions (Table 4). Kruskal–Wallis tests (turkey vulture: $\chi^2 = 187.1$, $P < 0.0001$; black vulture: $\chi^2 = 130.3$, $P < 0.0001$) and Dunn's multiple comparisons tests ($P < 0.05$) showed that median cell soma area was significantly different among the low, medium and high density retinal regions in both species. However, Mann–Whitney U-tests revealed that there were no significant differences between the two species in median cell soma area for the same retinal regions

TABLE 2. Results of stereological sampling of the retinal ganglion cell layer in three turkey vulture and three black vulture retinal whole mounts using the optical fractionator method

Species/Specimen ID	Eye	Post-stain whole mount area (mm²)	Sampling grid (mm)	Counting frame (μm)	Number of sample points	asf	Total number of cells	CE	Average cell density (cells mm⁻²)
Turkey vulture									
GRG4204	Right	584.9	1 × 1	35 × 35	553	0.001225	3,868,571	0.023	6,614
GRG4220	Left	610.7	1.3 × 1.3	35 × 35	333	0.0007249	3,826,988	0.026	6,267
GRG4235	Left	586.4	1.5 × 1.5	35 × 35	221	0.0005444	4,121,633	0.03	7,029
Average ± SD		594.0 ± 14.5			369 ± 169		3,939,064 ± 159,471	0.026 ± 0.004	6,637 ± 382
Black vulture									
GRG4195	Left	511.3	1 × 1	35 × 35	492	0.001225	3,870,204	0.018	7,145
GRG4196	Left	565.9	1.3 × 1.3	35 × 35	284	0.0007249	4,097,388	0.027	8,014
GRG4240	Left	541.6	1.3 × 1.3	35 × 35	320	0.0007249	3,450,359	0.029	6,098
Average ± SD		539.6 ± 27.4			365 ± 111		3,805,984 ± 328,260	0.02 ± 0.01	7,086 ± 960

asf: area sampling fraction, CE: coefficient of error.

(low density region: $U = 174{,}072$, $P = 0.32$; medium density region: $U = 174{,}940$, $P = 0.40$; high density region: $U = 177{,}701$, $P = 0.70$).

Spatial Resolving Power

Estimates of peak SRP were calculated for turkey and black vultures (Table 3), using the axial lengths (A) and peak cell densities obtained for each eye. SRP was calculated for the central foveate area and the temporal afoveate area in each retina. On average, we estimated peak SRP for the central area to be 15.4 cycles/deg in turkey vultures and 15.8 cycles/deg in black vultures. SRP for the temporal area was ∼2–3 cycles/deg lower in both species. There was no significant difference in SRP in turkey and black vultures for either the central area ($t = 0.26$, $df = 4$, $P = 0.81$) or the temporal area ($t = 0.18$, $df = 4$, $P = 0.87$).

DISCUSSION

Eye Morphology

Eyes, and their recipient visual brain areas, are energetically costly to build and maintain and use significant quantities of energy to process information (Laughlin, 2001a,b; Niven and Laughlin, 2008). Moreover, large eyes may incur additional costs, for example, by increasing mass or drag, which are important issues for flying animals (Brooke et al., 1999; Laughlin, 2001a). Therefore, the amount of investment in the visual system relative to other body parts should be more or less equivalent to the visual requirements of a species (Laughlin, 2001a; Niven and Laughlin, 2008). Eye size relative to body size has thus been used as an indicator of the relative importance of vision in birds (Ritland, 1982; Brooke et al., 1999; Garamszegi et al., 2002; Howland et al., 2004) as well as other animals (Ritland, 1982; Motani et al., 1999; Howland et al., 2004; Lisney and Collin, 2007). Here, we found that eye size relative to body mass was the same in black vultures and turkey vultures. Similarly, there was no significant difference in axial eye diameter (A) between the two species and although transverse eye diameter (T) was significantly larger in turkey vultures, this difference amounted to <1 mm. While an absolutely larger eye can result in a species having a greater SRP (as spatial resolution is proportional to the focal length of the eye; Brooke et al., 1999), we found no significant differences in peak SRP between the two vultures (see below).

Eye shape differed significantly between the two species; black vultures had relatively larger corneas than turkey vultures. This may indicate that black vultures have a greater visual sensitivity than turkey vultures, because a relatively larger cornea increases the eye's light gathering capability and species that are crepuscular or nocturnal have relatively larger corneas than diurnal species (Kirk, 2004, 2006a,b; Hall and Ross, 2007; Schmitz and Wainwright, 2011; Veilleux and Lewis, 2011; Lisney et al., 2012a,b, 2013). However, no differences in activity pattern have been reported between the two species, both of which are diurnal (Houston, 1986; del Hoyo et al., 1994) with occasional observations of nocturnal behavior (Tabor and McAllister, 1988; Mandell and Bildstein, 2007; Charette et al., 2011). In comparison with other birds, the *C:T* and *C:A* values for both
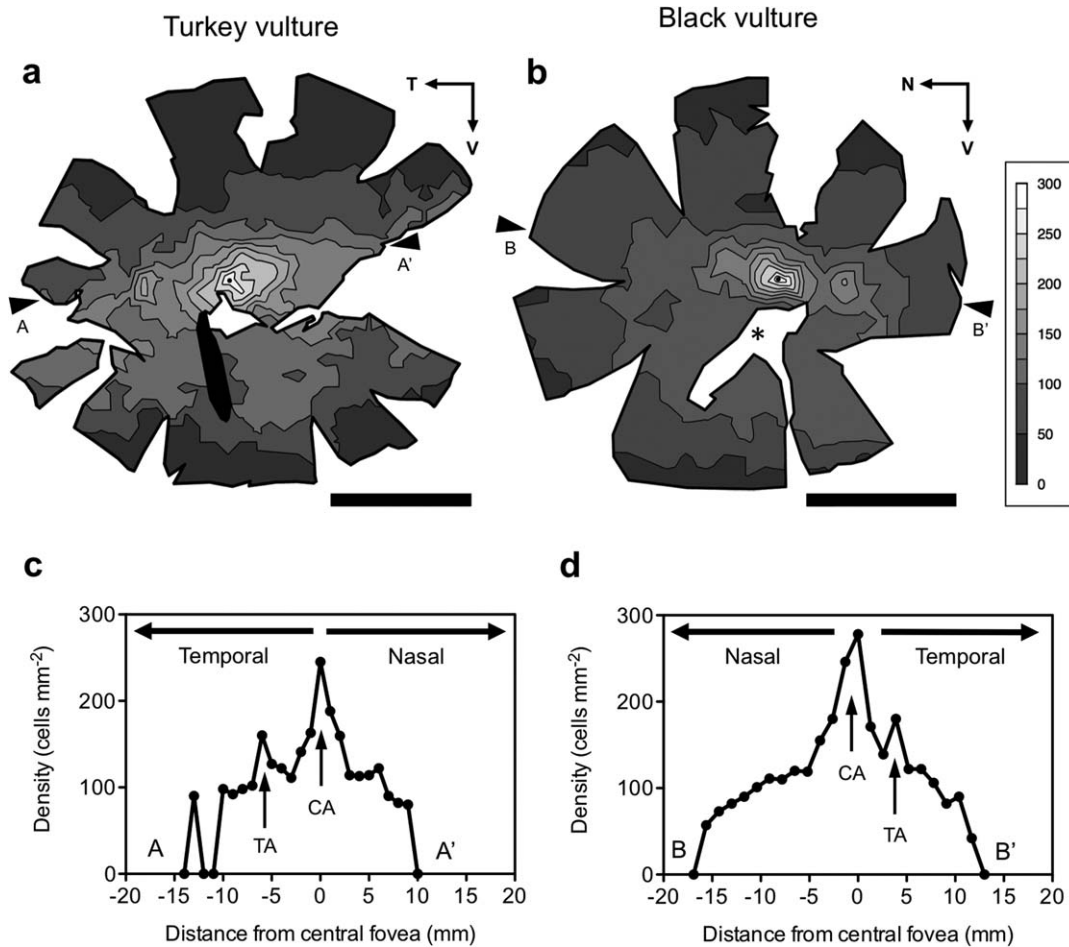
Fig. 5. Retinal topography in turkey vultures and black vultures. (a–b) Representative isodensity contour maps illustrating the topographic distribution of cells in the RGC layer in the two species. (a) Right retina from a turkey vulture (specimen ID: GRG4220). (b) Left retina from a black vulture (specimen ID: GRG4195). The shaded density scales, which are the same for both species, represent $\times 10^2$ cells mm^{-2}. The position of a fovea in the central high density area in a and b is shown as a small black dot within the highest density contour. The irregular black shape in a represents the position of the pecten, while in b the white area marked with an asterisk (*) indicates the position of the pecten, which for this retina was dissected out to allow the whole mount to lie flat. Scale bars represent 10 mm. N: nasal, T: temporal, V: ventral. (c–d) Density profiles for cells in the RGC layer measured along a temporal-nasal transect (A–A′) across the retina in the turkey vulture whole mount (c) and a nasal-temporal transect (B–B′) in the black vulture whole mount (d). The arrows in a and b mark the position of the transects, which run through the two high cell density areas in each retina, the central, foveate area (CA) and the temporal, afoveate area (TA). The density scale on the y-axes represents $\times 10^2$ cells mm^{-2}.

turkey and black vultures are well within the values previously documented for diurnal birds and are much lower than the ratios found in nocturnal species, such as kiwi (*Apteryx* sp.), kakapo (*Strigops habroptilus*) and some owls (Hall and Ross, 2007; Martin et al., 2007; Corfield et al., 2011; Lisney et al., 2012a, 2013). When taken in this context, the eyes of both vulture species are clearly adapted for diurnal vision and the differences in eye shape probably do not represent a substantial difference in visual abilities.

Cell Soma Area

The analysis of the soma area of cells in the RGC layer revealed a wide range of soma sizes. Because we did not differentiate between RGCs and displaced amacrine cells, it should be noted that some of the smaller cells included in the analysis of soma area are very

likely to have been amacrine cells (putative displaced amacrine cells in avian retinae are typically <20 µm^2; Ehrlich, 1981; Chen and Naito, 1999). However, it is not possible to simply classify all of the smallest cells as amacrine cells, because retrograde labeling studies have revealed that very small (≤ 20 µm^2) RGCs are present in avian retinas (Bravo and Pettigrew, 1981; Ikushima et al., 1986) and that the size ranges of amacrine cells and very small RGCs overlap (Hayes, 1984).

The wide range of soma sizes we found in the RGC layer in both species of vultures probably reflects the presence of a variety of different RGC classes, as in other birds (Bravo and Pettigrew, 1981; Ikushima et al., 1986; Naito and Chen, 2004; Lisney et al., 2012a). This includes a sub-population of large, sparsely distributed RGCs with two to four primary dendrites (Fig. 3). Although we did not quantify the morphology or the distribution of these cells in this study, we encountered

TABLE 3. Optical and anatomical parameters used to estimate theoretical peak anatomical spatial resolution of the central and temporal areas of high cell density in turkey and black vultures

Species/ specimen ID	Eye axial length (mm)	PND (mm)	Central, foveate area		Temporal, afoveate area	
			Peak cell density (cells mm^{-2})	SRP (cycles deg^{-1})	Peak cell density (cells mm^{-2})	SRP (cycles deg^{-1})
Turkey vulture						
GRG4204	19.5	11.7	18,776	15.0	16,000	13.9
GRG4220	18.5	11.1	24,490	16.3	16,327	13.3
GRG4235	18.7	11.22	20,408	15.0	15,347	13.0
Average ± SD	18.9 ± 0.53	11.34 ± 0.32	21,225 ± 2,943	15.4 ± 0.8	15,891 ± 499	13.4 ± 0.5
Black vulture						
GRG4195	18	10.8	20,408	14.5	18,776	13.9
GRG4196	17.96	10.78	27,755	16.8	17,959	13.5
GRG4240	18.64	11.18	23,224	16.0	15,347	13.0
Average ± SD	18.2 ± 0.38	10.92 ± 0.23	23,796 ± 3,707	15.8 ± 1.2	17,361 ± 1,791	13.5 ± 0.5

PND: posterior nodal distance, SRP: spatial resolving power.

these cells in the low density, and to a lesser extent, medium density regions of the retina in both species. These large cells appear to resemble the "giant ganglion cells," whose population has been described and mapped topographically in other birds (Hayes et al., 1991; Coimbra et al., 2006, 2009, 2012).

The soma area frequency distributions were similar for both species, which is consistent with Inzunza et al.'s (1991) observations for black vultures and Andean condors. It is therefore likely that the proportions of different RGC classes are largely the same across all cathartid vultures, regardless of their propensity to use visual or olfactory cues. However, we also acknowledge that a far more detailed study would be required to identify specific morphological RGC classes in vultures. For example, distinguishing cells based on soma field size as well as arborization and stratification in the inner plexiform layer of the dendrites (e.g., Ikushima et al., 1986; Sun et al., 2002; Naito and Chen, 2004; Pushchin and Karetin, 2009) would aid in determining whether the number or distribution of these RGC classes varies among species.

We also found that cell soma area is inversely proportional to cell density in the RGC layer of turkey and black vultures. The small, more densely-packed cells in the central regions of the retina are relatively more homogeneous in size compared to those in the low-density retinal periphery. This pattern is consistent with previous findings for diurnal birds of prey, including cathartids (Inzunza et al., 1991), and for birds in general (Ehrlich, 1981; Hayes and Brooke, 1990; Chen and Naito, 1999; Boire et al., 2001; Dolan and Fernández-Juricic, 2010; Lisney et al., 2012a, 2013).

Retinal Topography

The overall retinal topography, along with our estimates of the total number of cells in the RGC layer, peak and average cell densities, cell soma area frequency distributions, and peak SRP was the same in turkey and black vultures. Our results for black vultures are consistent with those of Inzunza et al. (1991) and the identification of a central fovea in turkey vultures corroborates Lord (1956). On the basis of our results,

TABLE 4. Summary of cell soma measurements made from 200 cells in each of three retinal regions (of "low," "medium," and "high" density) for each of the six vulture whole mounts (three per species) analyzed in this study

Whole mount region	Parameter	Turkey vulture; *Cathartes aura*	Black vulture; *Coragyps atratus*
"Low" density (<10,000 cells mm^{-2})	Number of cells measured	600	600
	Median cell soma area (μm^2)	35.8	30.17
	25–75% percentiles (μm^2)	24.1–64.8	22.3–77.5
	Overall cell soma area range (μm^2)	14.1–342.1	15.7–448.1
"Medium" density (10,000–14,999 cells mm^{-2})	Number of cells measured	600	600
	Median cell soma area (μm^2)	29.8	27.5
	25–75% percentiles (μm^2)	20.5–48.6	19.7–49.7
	Overall cell soma area range (μm^2)	13.9–234.4	9.5–259.9
"High" density (≥15,000 cells mm^{-2})	Number of cells measured	600	600
	Median cell soma area (μm^2)	23.6	24.0
	25–75% percentiles (μm^2)	17.8–32.6	18.8–31.3
	Overall cell soma area range (μm^2)	10.5–114.6	11.1–237.0

Because of the skewed nature of the cell soma area frequency distributions (Fig. 6), median values are presented in preference to averages.

there appear to be few anatomical differences in retinal topography between the two vultures, at least at the level of the RGCs.

Both vulture species are found in a variety of habitats, ranging from open prairie and savanna grassland to neotropical rain forest (Houston, 1987; del Hoyo et al., 1994; Ferguson-Lees and Christie, 2001). The ability of turkey vultures to detect food by olfaction alone appears to be particularly beneficial in forested habitats when carcasses are visually obscured by foliage (Houston, 1984, 1986, 1988; Ferguson-Lees and Christie, 2001). In closed-canopy habitats, black vultures are at a disadvantage because they cannot directly locate carcasses by sight while soaring and so they often rely on following turkey vultures (or other *Cathartes* species) to carcasses (Houston, 1986; del Hoyo et al., 1994; Buckley, 1996; Stolen, 2000). In open habitats where carcasses are not obscured, black vultures use vision to locate carcasses, but also follow other vultures to carcasses. However, in these same open habitats, turkey vultures may also rely on visual cues, or a combination of visual and olfactory cues, to locate food (Lord, 1956; Owre and Northington, 1961). Indeed, Smith and Paselk (1986) have cast some doubt on the importance of olfaction alone in detection of the carcasses of the small-bodied animals that turkey vultures appear to prefer, which in turn implies a role for other sensory modalities (i.e., vision). In addition to a role in the detection and localization of carcasses, vision may also be important for other tasks such as navigation and obstacle avoidance and social behavior in both species.

The pattern of retinal specializations we have described for turkey and black vultures has previously been reported for black vultures, Andean condors (Inzunza et al., 1989, 1991) and for diurnal birds of prey in general (Slonaker, 1897; Wood, 1917; Fite and Rosenfield-Wessels, 1975; Inzunza et al., 1989, 1991) (not including diurnal owls; Lisney et al., 2012a). The presence of specific areas of high cell density in the central and temporal parts of the retina suggests that the frontal-lateral visual field (central high density area) and the frontal visual field (temporal high density area) are of particular importance to these birds, whether they are predators or scavengers. Although we did not specifically assess retinal topography in relation to the visual fields in either vulture species, evidence from other studies on diurnal birds of prey suggests that the fovea in the central high density area is associated with the fronto-lateral part of the visual field whereas the temporal high density area is associated with the frontal visual field, closer to the midline (Slonaker, 1897; Lord, 1956; Tucker, 2000).

Despite the similarities in retinal topography among diurnal birds of prey, there are some major differences in retinal organization between predatory species and scavengers. First, predatory species exhibit much higher numbers and densities of cells in the RGC layer; kestrels and hawks have peak cell densities 2.5–4.0 times greater than that of the turkey and black vultures (Table 5). The chimango caracara (*Milvago chimango*), a species of raptor that forages on the ground and eats a relatively large amount of carrion (del Hoyo et al., 1994; Ferguson-Lees and Christie, 2001), has a peak RGC density that falls between those of entirely predatory species and the scavenging vultures (Inzunza et al., 1991). Second, predatory diurnal birds of prey are bifoveate, with foveae in both the central and temporal areas of the retina (Slonaker, 1897; Wood, 1917; Lord, 1956; Fite and Rosenfield-Wessels, 1975; Inzunza et al., 1989, 1991), but only the central area is foveated in scavengers (Walls, 1942; Lord, 1956; Inzunza et al., 1989, 1991). Foveae are specializations for acute vision (Slonaker, 1897; Walls, 1942; Fite and Rosenfield-Wessels, 1975; Meyer, 1977) and so this difference presumably reflects the differential visual requirements of predatory and scavenging raptors. More specifically, both predatory and scavenging species use the central fovea for viewing distant objects monocularly with a high SRP, but predatory species also require a temporal fovea for viewing objects binocularly with a high SRP, albeit slightly lower than that of the central fovea (Lord, 1956; Frost et al., 1990; Tucker, 2000). This temporal fovea probably serves an important role in prey capture in predatory species (Martin and Katzir, 1999; O'Rourke et al., 2010) that is not required by scavenging species.

Spatial Resolving Power

In this study, we have estimated SRP using the peak density of cells in the RGC layer and an estimate of focal length. The RGCs and their axons represent the only link between the eye and the brain and thus the spatial distribution of the RGCs places an upper limit on SRP (Hughes, 1977; Pettigrew et al., 1988; Collin and Pettigrew, 1989). In species where SRP has been determined anatomically and behaviorally, the two measures are in close agreement and are highly correlated with one another (Reymond, 1985; Kiltie, 2000; Pettigrew et al., 1988; Pettigrew and Manger, 2008).

The RGC layer contains both the RGCs and displaced amacrine cells. In this study, we counted all the Nissl-stained cells in the RGC layer, which means that the displaced amacrine cell population has been included in our data. Therefore, we accept that the cell counts represent an overestimation of the true RGC densities (due to the inclusion of the displaced amacrine cells). However, we do not consider this to be a major issue for two important reasons. First, in a range of species from various vertebrate groups (including fishes, reptiles, birds, and mammals) for which RGC topography has been assessed using both Nissl staining and retrograde-labeling from the optic nerve or retino-recipient areas in the brain (in order to exclusively label RGCs), both the peak cell densities and the overall topographic distribution of cells remain relatively similar, despite the inclusion of the displaced amacrine cells (Peterson and Ullinski, 1979; Bravo and Pettigrew, 1981; Collin, 1988; Collin and Pettigrew, 1988; Pettigrew et al., 1988; Chen and Naito, 1999; Bailes et al., 2006). Second, cell counts from the RGC layer are converted to cell density (i.e., cell mm^{-2}) and then reduced to the square root for the purposes of calculating SRP, meaning that a relatively large difference in peak cell density values results in a small difference in terms of SRP (Pettigrew et al., 1988; Pettigrew and Manger, 2008; Ullman et al., 2012). In this study, despite the inclusion of amacrine cells, we found that our peak cell density values for the central and temporal high density areas for the black vulture (Table 3) are very similar to those reported by Inzunza et al. (1991), who did differentiate between RGCs and amacrine cells. Moreover, there is evidence that in the

TABLE 5. A comparison of theoretical peak anatomical spatial resolving power (SRP) in the central and temporal areas of high cell density in predatory and scavenging diurnal birds of prey

Species	Common name	Feeding mode	Eye axial length (mm)	PND (mm)	Central high density area Peak cell density (cells mm^{-2})	SRP (cycles deg^{-1})	Temporal high density area Peak cell density (cells mm^{-2})	SRP (cycles deg^{-1})
Sturnus vulgaris	European starling	Omnivore	7.7[a]	4.6[b]	25,317[a]	6.3[a]	–	–
Milvago chimango	Chimango caracara	Predator/ scavenger	8.6[c]	5.2[b]	38,000[d]	9.4	23,000[d]	7.4
Coturnix japonica	Japanese quail	Granivore	9.3[e]	5.6[e]	35,115[e]	9.7[e]	–	–
Columba livia	Pigeon	Granivore	–	7.9[f]	41,000[g]	15.0	36,000[g]	14.1
Cathartes aura	Turkey vulture	Scavenger	18.9[h]	11.34[b]	21,225[h]	15.4	15,891[h]	13.4
Coragyps atratus	Black vulture	Scavenger	18.2[h]	10.92[b]	25,000[d]; 23,796[h]	16.2; 15.8	16,000[d]; 17,361[h]	13.0; 13.5
Branta canadensis	Canada goose	Granivore/ herbivore	21.0[e]	12.6[e]	20,400[e]	16.9	–	–
Falco sparverius	American kestrel	Predator	13.2[c]	7.9[b]	107,220[i]; 65,000[d]	24.3; 18.9	65,361[i]; 45,000[d]	18.9; 15.7
Vultur gryphus	Andean condor	Scavenger	23.7[c]	14.2[b]	35,000[d]	24.9	20,000[d]	18.8
Geranoaetus melanoleucus	Black-chested buzzard-eagle	Predator	22.0[j]	13.2[b]	62,000[d]	30.8	45,000[d]	26.3
Accipiter gentilis	Northern goshawk	Predator	22.3[c]	13.4[b]	67,712[i]	32.7	42,868[i]	26.0
Buteo jamaicensis	Red-tailed hawk	Predator	27.3[c]	16.4[b]	99,077[i]	48.4	72,034[i]	41.3

Four species of ground-feeding bird with different feeding modes (herbivory, granivory and omnivory) have also been included for comparison. SRP was calculated using peak cell densities in the retinal ganglion cell layer and posterior nodal distance (PND) as measure of the focal length of each eye, following the approach of Hart (2002).

Sources of information:
[a]Dolan and Fernández-Juricic (2010).
[b]Calculated assuming PND is ×0.6 of the eye axial length (Hughes, 1977; Martin, 1994; Ullmann et al., 2012).
[c]Ritland (1982).
[d]Inzunza et al. (1991).
[e]Lisney et al. (2012b).
[f]Marshall et al. (1973).
[g]Hayes and Holden (1983).
[h]This study.
[i]Calculated using values presented in table 2 of Fite and Rosenfield-Wessels (1975).
[j]Used average value from Ritland (1982) for eagles (genus *Buteo*), to which the black-chested buzzard-eagle is closely related (Riesing et al., 2003).
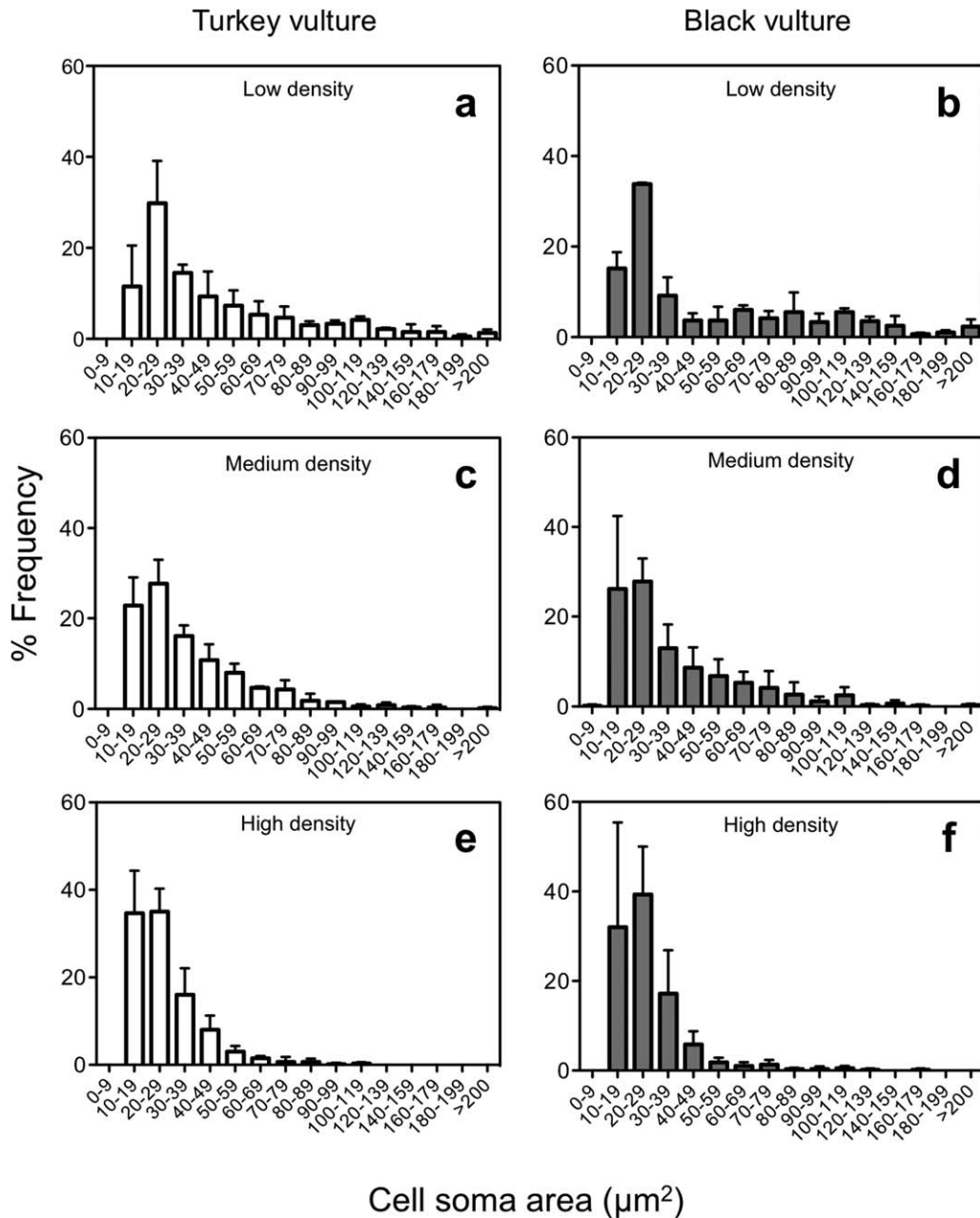
Turkey vulture   Black vulture

Cell soma area (µm²)

Fig. 6. Cell soma area (µm²) versus % frequency histograms of cells located in low- (<10,000 cells mm⁻²) (a–b), medium- (10,000–14,999 cells mm⁻²) (c–d) and high- (≥15,000 cells mm⁻²) (e–f) density regions of the RGC layer in turkey vultures (white: a, c, e) and black vultures (grey: b, d, f). 200 cells were measured in each of the three retinal regions for each of the three whole mounts used for both species. Error bars represent ±SD.

central foveal region in diurnal birds of prey, <1% of cells are amacrine cells (Inzunza et al., 1991). Therefore, we are confident that our peak cell density values are representative of the peak RGC densities.

SRP for both the central and temporal high density areas was very similar in turkey and black vultures (Table 3), which suggests that their visual acuity is similar even though they frequently fly at different altitudes when foraging (see Introduction). As mentioned previously, rigorously quantified data on foraging height are

lacking for these species. However, foraging turkey vultures have been reported to often fly within 30 m of the ground, while black vultures fly at higher altitudes of 300 m (Houston, 1988; Buckley, 1996). Therefore, following the methods described in Marshall (2000), we calculated the size of the smallest objects that would theoretically be resolvable from these heights, as viewed with an eye with a SRP of 15.6 cycles/deg, which is the overall average SRP we calculated for the central high density area for both species (using data presented in

Table 3). At 30 m, objects up to 33 mm would be resolvable, while at 300 m, the smallest resolvable object would be ~33.5 cm. We also calculated the altitude at which a 2 m object would become unresolvable. We did this in order to compare our estimates of SRP in turkey and black vultures with Spiegel et al.'s (2013) estimates of SRP for two species of Old World vulture, lappet-faced vultures (*Torgos trachelio*tus) and white-backed vultures (*Gyps africanus*). With a SRP of 15.6 cycles/deg, a 2 m object would theoretically become unresolvable at an altitude of ~1790 m. This contrasts with over 10,000 m and 6,500 m for the lappet-faced and white-backed vultures, respectively (Spiegel et al., 2013). We suspect that this enormous discrepancy does not reflect a true difference in the visual capabilities between Old and New World vultures. This is because, unlike us, Spiegel et al. (2013) did not directly assess eye size or retinal organization in lapped-faced or white-backed vultures in order to calculate SRP, but instead used previously published scaling relationships based on avian and mammalian eyes. Thus we believe our estimates of SRP for turkey and black vultures are likely much more realistic than those presented by Spiegel et al.'s (2013), although a lack of data on the eyes and retinas of Old World vultures (see below) prevents us from confirming this.

Our estimates of peak SRP for the two vulture species are much lower than those calculated using the same methods for predatory diurnal birds of prey with comparably-sized or larger eyes (Table 5). Most notably, peak SRP in the two vulture species is almost 10× lower than that of wedge-tailed eagles (*Aquila audax*) (ca., 140 cycles/deg) as determined anatomically using cone photoreceptor spacing in the central fovea and verified behaviorally (Reymond, 1985). For comparison, peak SRP in humans is ~50–60 cycles/deg (Campbell, 1965; Hughes, 1977; Pettigrew et al., 1988; Pettigrew and Manger, 2008). Because eye size has a significant effect on SRP (Brooke et al., 1999; Ullman et al., 2012), the differences in SRP between turkey and black vultures and the smaller-eyed American kestrel (*Falco sparverius*) are smaller (Table 5). Diurnal birds of prey, including vultures, have long been considered to have excellent visual acuity (e.g., Knox, 1826; Slonaker, 1897; Walls, 1942; Lord, 1956; Meyer, 1977; Reymond, 1985; Ferguson-Lees and Christie, 2001; Houston, 2001). On the basis of our data, however, the assumption that visual acuity in turkey and black vultures is in anyway equivalent to predatory diurnal birds of prey should be called into question. Indeed, our estimates of peak SRP for the turkey and black vultures are comparable with those reported for the Canada goose (*Branta canadensis*) and the pigeon (*Columba livia*), although they are generally higher than those of other ground-feeding birds, such as the Japanese quail (*Coturnix japonica*) and the European starling (*Sturnus vulgaris*) (Table 5).

The differences in SRP among diurnal birds of prey reflect the peak RGC density (as described above) and are presumably related to differing visual demands associated with scavenging and predation. However, despite also having a relatively low peak RGC density (Inzunza et al., 1991), Andean condors, another scavenging cathartid species, have a SRP more comparable to those found in predatory species (Table 5). This is on account of these birds having a much larger eye than the other vultures and thus a greater PND. Having a higher

degree of spatial resolution may be particularly beneficial to Andean condors because they cover very large areas in search of carrion and must spot carcasses from afar (Wallace and Temple, 1987b). Unfortunately, no information on retinal topography and SRP is currently available for any species of Old World vultures (Accipitridae). The phylogenetic relationship between New World and Old World vultures remains controversial. Some recent studies indicate that these two groups are closely related (Hackett et al., 2008; Jetz et al., 2012), whereas a number of other studies suggest that they belong to different orders (Seibold and Helbig, 1995; Wink, 1995; Livezey and Zusi, 2007; Tagliarini et al., 2009; Ericson, 2012). However, even in studies that suggest a close relationship between the two clades, New and Old world vultures do not form a monophyletic clade (Hackett et al., 2008; Jetz et al., 2012). Thus, these two groups of vultures share numerous anatomical, physiological, and behavioral adaptations to a scavenging niche through convergent evolution and not homoplasy (Wink, 1995; Houston, 2001). If a lower SRP than predatory species and a single, central fovea are all common characteristics of scavenging birds of prey, we expect that the Old World vultures will have a similar retinal topography, eye shape and SRP to that described for New World vultures.

ACKNOWLEDGEMENTS

LITERATURE CITED

Ahnelt PK, Schubert C, Kübber-Heiss A, Schiviz A, Anger E. 2006. Independent variation of retinal S and M cone photoreceptor topographies: a survey of four families of mammals. Vis Neurosci 23: 429–435.

Bailes HJ, Trezise AEO, Collin SP. 2006. The number, morphology, and distribution of retinal ganglion cells and optic axons in the Australian lungfish *Neoceratodus forsteri* (Krefft 1870) Vis Neurosci 23:257–273.

Bang BG. 1964. The nasal organs of the black and turkey vultures: a comparative study of the cathartid species *Corayps atratus aratus* and *Cathares aura septentrionalis* (with notes on Cathartes aura falkandica, *Pseudogyps bengalensis* and *Neophron percnopterus*). J Morph 115:153–184.

Bang BG, Cobb S. 1968. The size of the olfactory bulb in 108 species of birds. Auk 85:55–61.

Beasley JC, Olson ZH, DeVault TL. 2012. Carrion cycling in food webs: comparisons among terrestrial and marine ecosystems. Oikos 121:1021–1026.

Boire D, Dufour JS, Theoret H, Ptito M. 2001. Quantitative analysis of the retinal ganglion cell layer in the ostrich, *Struthio camelus*. Brain Behav Evol 58:343–355.

Bravo H, Pettigrew JD. 1981. The distribution of neurons projecting from the retina and visual cortex to the thalamus and tectum

opticum of the barn owl, *Tyto alba*, and burrowing owl, *Speotyto cunicularia*. J Comp Neurol 199:419–441.

Brooke M de L, Hanley S, Laughlin SB. 1999. The scaling of eye size with body mass in birds. Proc R Soc Lond B 266:405–412.

Buckley NJ. 1996. Food finding and the influence of information, local enhancement, and communal roosting on foraging success of North American vultures. Auk 113:473–488.

Campbell FW. 1965. Optical and retinal factors affecting visual resolution. J Physiol 181:576–593.

Charette MR, Pelletier F, Calmé S. 2011. Observation of nocturnal feeding in black vultures (*Coragyps atratus*). J Raptor Res 45:279–280.

Chen Y, Naito J. 1999. A quantitative analysis of the cells in the ganglion cell layer of the chick retina. Brain Behav Evol 53:75–86.

Coimbra JP, Marceliano MLV, Andrade-da-Costa BLS, Yamada ES. 2006. The retina of tyrant flycatchers: topographic organization of neuronal density and size in the ganglion cell layer of the great kiskadee *Pitangus sulphuratus* and the rusty margined flycatcher *Myiozetetes cayanensis* (Aves: Tyrannidae). Brain Behav Evol 68:15–25.

Coimbra JP, Nolan PM, Collin SP, Hart NS. 2012. Retinal ganglion cell topography and spatial resolving power in penguins. Brain Behav Evol 80:254–268.

Coimbra JP, Trévia N, Marceliano ML, da Silveira Andrade-Da-Costa BL, Picanço-Diniz CW, Yamada ES. 2009. Number and distribution of neurons in the retinal ganglion cell layer in relation to foraging behaviors of tyrant flycatchers. J Comp Neurol 514:66–73.

Collin SP. 1988. The retinae of the shovel-nosed ray, *Rhinobatos batillum* (Rhinobatidae): morphology and quantitative analysis of the ganglion, amacrine and bipolar cell populations. Exp Biol 47:195–207.

Collin SP, Pettigrew JD. 1988. Retinal ganglion cell topography in teleosts: a comparison between Nissl-stained material and retrograde labelling from the optic nerve. J Comp Neurol 276:412–422.

Collin SP, Pettigrew JD. 1989. Quantitative comparisons of the limits on visual spatial resolution set by the ganglion cell layer in twelve species of reef teleosts. Brain Behav Evol 34:184–192.

Corfield JR, Gsell AC, Brunton D, Heesy CP, Hall MI, Acosta ML, Iwaniuk AN. 2011. Anatomical specializations for nocturnality in a critically endangered parrot, the kakapo (*Strigops habroptilus*). PLoS ONE 6:e22945.

del Hoyo J, Elliott A, Sargatal J. 1994. Handbook of the birds of the world. Vol. II. New World Vultures to Guineafowl. Barcelona: Lynx Edicions.

DeVault TL, Rhodes OE, Jr, Shivik JA. 2003. Scavenging by vertebrates: behavioral, ecological, and evolutionary perspectives on an important energy transfer pathway in terrestrial ecosystems. Oikos 102:225–234.

DeVault TL, Olson ZH, Beasley JC, Rhodes OE, Jr. 2011. Mesopredators dominate competition for carrion in an agricultural landscape. Basic Appl Ecol 12:268–274.

Dolan T, Fernández-Juricic E. 2010. Retinal ganglion cell topography of five species of ground-foraging birds. Brain Behav Evol 75:111–121.

Ehrlich D. 1981. Regional specialization of the chick retina as revealed by the size and density of neurons in the ganglion cell layer. J Comp Neurol 195:643–657.

Ericson PGP. 2012. Evolution of terrestrial birds in three continents: biogeography and parallel radiations. J Biogeogr 39:813–824.

Ferguson-Lees J, Christie DA. 2001. Raptors of the world. New York: Houghton Mifflin.

Fite KV, Rosenfield-Wessels S. 1975. A comparative study of deep avian foveas. Brain Behav Evol 12:97–115.

Frost BJ, Wise LZ, Morgan B, Bird D. 1990. Retinotopic representation of the bifoveate eye of the kestrel (*Falco sparverius*) on the optic tectum. Vis Neurosci 5:231–239.

Garamszegi LZ, Møller AP, Erritzøe J. 2002. Coevolving avian eye size and brain size in relation to prey capture and nocturnality. Proc R Soc Lond B 269:961–967.

Gomez LG, Houston DC, Cotton P, Tye A. 1994. The role of greater yellow-headed vultures *Cathartes melambrotus* as scavengers in neotropical forest. Ibis 136:193–196.

Graves GR. 1992. Greater yellow-headed vulture (*Cathartes melambrotus*) locates food by olfaction. J Raptor Res 26:38–39.

Gundersen HJG. 1977. Notes on the estimation of the numerical density of arbitrary particles: the edge effect. J Microsc 111:219–223.

Gunter H, Myer A. 2013. Trade-offs in cavefish sensory capacity. BMC Biol 11:5.

Hackett SJ, Kimball RT, Reddy S, Bowie RCK, Braun EL, Braun MJ, Chojnowski JL, Cox WA, Han K-L, Harshman J, Huddleston CJ, Marks BD, Miglia KJ, Moore WS, Sheldon FH, Steadman DW, Witt CC, Yuri T. 2008. A phylogenomic study of birds reveals their evolutionary history. Science 320:1763–1768.

Hall MI, Ross CF. 2007. Eye shape and activity pattern in birds. J Zool 271:437–444.

Hart NS. 2002. Vision in the peafowl (Aves: *Pavo cristatus*). J Exp Biol 205: 3925–3935.

Hart NS, Coimbra JP, Collin SP, Westhoff G. 2012. Photoreceptor types, visual pigments, and topographic specializations in the retinas of hydrophilid sea snakes. J Comp Neurol 520:1246–1261.

Hayes BP. 1984. Cell populations of the ganglion cell layer: displaced amacrine and matching amacrine cells in the pigeon retina. Exp Brain Res 56:565–573.

Hayes BP, Brooke ML. 1990. Retinal ganglion cell distribution and behavior in procellariiform seabirds. Vis Res 30:1277–1289.

Hayes BP, Holden AL. 1983. The distribution of displaced ganglion cells in the retina of the pigeon. Exp Brain Res 49:181–188.

Hayes BP, Martin GR, Brooke ML. 1991. Novel area serving binocular vision in the retinae of procellariform seabirds. Brain Behav Evol 37:79–84.

Houston DC. 1984. Does the King Vulture *Sarcoramphus papa* use a sense of smell to locate food? Ibis 126:67–69.

Houston DC. 1986. Scavenging efficiency of turkey vultures in tropical forest. Condor 88:318–323.

Howland HC, Merola S, Basarab JR. 2004. The allometry and scaling of the size of vertebrate eyes. Vis Res 44:2043–2065.

Houston DC. 1987. The effect of reduced mammal numbers on *Cathartes* vultures in Neotropical forests. Biol Cons 41:91–98.

Houston DC. 1988. Competition for food between Neotropical vultures in forest. Ibis 130:402–417.

Houston DC. 2001. Condors and vultures. Stillwater: Voyageur Press.

Hughes A. 1977. The topography of vision in mammals of contrasting lifestyles: comparative optics and retinal organization. In: Cresitelli F, editor. Handbook of sensory physiology. Vol. VIII/5. Berlin: Springer-Verlag. p 613–756.

Hughes A. 1985. New perspectives in retinal organization. In: Osbourne NN, Chader G, editors. Progress in retinal research. New York: Pergamon Press. p 243–313.

Ikushima M, Watanabe M, Ito H. 1986. Distribution and morphology of retinal ganglion cells in the Japanese quail. Brain Res 376:320–334.

Inzunza O, Bravo H, Smith RL. 1989. Foveal regions of bird retinas correlate with the aster of the inner nuclear layer. Anat Rec 223:342–346.

Inzunza O, Bravo H, Smith RL, Angel M. 1991. Topography and morphology of retinal ganglion cells in Falconiforms: a study on predatory and carrion-eating birds. Anat Rec 229:271–277.

Iwaniuk AN, Heesy CP, Hall MI. 2010. Morphometrics of the eyes and orbits of the nocturnal swallow-tailed gull (*Creagrus furcatus*). Can J Zool 88:855–865.

Jetz W, Thomas GH, Joy JB, Hartmann K, Mooers AO. 2012. The global diversity of birds in space and time. Nature 491:444–448.

Kiltie RA. 2000. Scaling of visual acuity with body size in mammals and birds. Funct Ecol 2000;14:226–234.

Kirk EC. 2004. Comparative morphology of the eye in primates. Anat Rec 281A:1095–1103.

Kirk EC. 2006a. Eye morphology in cathemeral lemurids and other mammals. Folia Primatol 77:27–49.

Kirk EC. 2006b. Effects of activity pattern on eye size and orbital aperture size in primates. J Hum Evol 51:159–170.

Knox R. 1826. II Observations on the comparative anatomy of the eye. Trans R Soc Edinb 10:43–78.

Laughlin SB. 2001a. The metabolic cost of information—a fundamental factor in visual ecology. In: Barth FG, Schmid A, editors. Ecology of sensing. Berlin: Springer-Verlag. p 169–186.

Laughlin SB. 2001b. Energy as a constraint on the coding and processing of sensory information. Curr Opin Neurobiol 11:475–480.

Lessells CM, Boag PT. 1987. Unrepeatable repeatabilities: a common mistake. Auk 104:116–121.

Lisney TJ, Collin SP. 2007. Relative eye size in elasmobranchs. Brain Behav Evol 69:266–279.

Lisney TJ, Collin SP. 2008. Retinal ganglion cell distribution and spatial resolving power in elasmobranchs. Brain Behav Evol 72:59–77.

Lisney TJ, Iwaniuk AN, Bandet MV, Wylie DW. 2012a. Eye shape and retinal topography in owls (Aves: Strigiformes). Brain Behav Evol 79:218–236.

Lisney TJ, Iwaniuk AN, Kolominsky J, Bandet MV, Corfield JR, Wylie DW. 2012b. Interspecifc variation in eye shape and retinal topography in seven species of galliform bird (Aves: Galliformes: Phasianidae). J Comp Physiol A 198:717–731.

Lisney TJ, Stecyk K, Kolominsky J, Schmidt BK, Corfield JR, Iwaniuk AN, Wylie DW. 2013. Ecomorphology of eye shape and retinal topography in waterfowl (Aves: Anseriformes: Anatidae) with different foraging modes. J Comp Physiol A 199:385–402.

Livezey BC, Zusi RL. 2007. Higher-order phylogeny of modern birds (Theropoda, Aves: Neornithes) based on comparative anatomy. II. Analysis and discussion. Zool J Linn Soc 149:1–95.

Livingston ME. 1987. Morphological and sensory specializations of five New Zealand flatfish species, in relation to feeding behaviour. J Fish Biol 31:775–795.

Lord RD, Jr. 1956. A comparative study of the eyes of some Falconiform and Passeriform birds. Am Midl Nat 56:325–344.

Mandell JT, Bildstein KL. 2007. Turkey vultures use anthropogenic thermals to extend their daily activity period. Wilson J Ornithol 119:102–105.

Marshall J, Mellerio J, Palmer DA. 1973. A schematic eye for the pigeon. Vis Res 13:2449–2453.

Marshall NJ. 2000. Communication and camouflage with the same "bright" colors in reef fishes. Phil Trans R Soc B 355:1243–1248.

Martin GR. 1994. Form and function in the optical structure of bird eyes. In: Davies MNO, Green PR, editors. Perception and Motor Control in Birds. Berlin: Springer-Verlag. p 5–34.

Martin GR. 2011. Understanding bird collisions with man-made objects: a sensory ecology approach. Ibis 153:239–254.

Martin GR, Katzir G. 1999. Visual fields in short-toed eagles, *Circaetus gallicus* (Accipitridae), and the function of binocularity in birds. Brain Behav Evol 53:55–66.

Martin GR, Piersma T. 2008. Vision and touch in relation to foraging and predator detection: insightful contrasts between a plover and a sandpiper. Proc R Soc Lond B 276:437–445.

Martin GR, Portugal SJ, Murn CP. 2012. Visual fields, foraging and collision vulnerability in Gyps vultures. Ibis 154:626–631.

Martin GR, Wilson K-J, Wild JM, Parsons S, Kubke MF, Corfield J. 2007. Kiwi forego vision in the guidance of their nocturnal activities. PLoS ONE 2:e198.

Meyer DB. 1977. The avian eye and its adaptations. In: Cresitelli F, editor. Handbook of sensory physiology. Vol. VIII/5. Berlin: Springer-Verlag. p 549–611.

Moore BA, Kamilar JM, Collin SP, Bininda-Emonds ORP, Dominy NJ, Hall MI, Heesy CP, Johnsen S, Lisney TJ, Loew ER, Moritz G, Nava SS, Warrant E, Yopak KE, Fernández-Juricic E. 2012. A novel method for comparative analysis of retinal specialization traits from topographic maps. J Vis 12:13.

Moroney MK, Pettigrew JD. 1987. Some observations on the visual optics of kingfishers (Aves, Coraciiformes, Alcedinidae). J Comp Physiol A 160:137–149.

Motani R, Rothschild BM, Wahl W, Jr. 1999. Large eyeballs in diving ichthyosaurs. Nature 402:747.

Naito J, Chen Y. 2004. Morphologic analysis and classification of ganglion cells of the chick retina by intracellular injection of lucifer yellow and retrograde labeling with DiI. J Comp Neurol 469:360–376.

Niven JE, Laughlin SB. 2008. Energy limitation as a selective pressure on the evolution of sensory systems. J Exp Biol 211:1792–1804.

O'Rourke CT, Hall MI, Pitlik T, Fernández-Juricic E. 2010. Hawk eyes I: diurnal raptors differ in visual fields and degree of eye movement. PLoS ONE 5:e12802.

Owre OT, Northington PO. 1961. Indication of the sense of smell in the turkey vulture, *Cathartes aura* (Linnaeus), from feeding tests. Am Midl Nat 66:200–205.

Peterson EH, Ulinski PS. 1979. Quantitative studies of retinal ganglion cells in a turtle, *Pseudemys scripta elegans*. 1. Number and distribution of ganglion cells. J Comp Neurol 186:17–42.

Pettigrew JD, Dreher B, Hopkins CS, McCall MJ, Brown M. 1988. Peak density and distribution of ganglion cells in the retinae of microchiropteran bats: implications for visual acuity. Brain Behav Evol 32:39–56.

Pettigrew JD, Manger PR. 2008. Retinal ganglion cell density of the black rhinoceros (*Diceros bicornis*): calculating visual resolution. Vis Neurosci 25:215–220.

Pettigrew JD, Manger PR, Fine SLB. 1998. The sensory world of the platypus. Phil Trans R Soc Lond B Biol Sci 353:1199–1210.

Prior KA, Weatherhead PJ. 1991. Competition at the carcass: opportunities for social foraging by turkey vulture in southern Ontario. Can J Zool 69:1550–1556.

Pushchin II, Karetin YA. 2009. Retinal ganglion cells in the eastern newt *Notophthalmus viridescens*: topography, morphology, and diversity. J Comp Neurol 516:533–552.

Rajchard J. 2008. Exogenous chemical substances in bird perception: a review. Vet Med-Czech 53:412–419.

Rasband WS. 1997–2012. Image J. US National Institutes of Health, Bethesda, MD, USA, Available at: http://imagej.nih.gov/ij/, 1997–2012.

Reymond L. 1985. Spatial visual acuity of the eagle *Aquila audax*: a behavioral, optical and anatomical investigation. Vis Res 25:1477–1491.

Riesing M, Kruckenhauser L, Gamauf A, Haring E. 2003. Molecular phylogeny of the genus *Buteo* (Aves: Accipitridae) based on mitochondrial marker sequences. Mol Phylogenet Evol 27:328–342.

Ritland S. 1982. The allometry of the vertebrate eye. PhD thesis. Chicago: University of Chicago.

Schaeffer RL, Mendenhall W, Ott L. 1996. Elementary survey sampling, 5th ed. Boston: PWS–Kent.

Schiviz AN, Ruf T, Kuebber-Heiss A, Schubert C, Ahnelt PK. 2008. Retinal cone topography of artiodactyl mammals: influence of body height and habitat. J Comp Neurol 507:1336–1350.

Schmitz C, Hof PR. 2000. Recommendations for straightforward and rigorous methods of counting neurons based on a computer simulation approach. J Chem Neuroant 20:93–114.

Schmitz L, Wainwright PC. 2011. Nocturnality constrains morphological and functional diversity in the eyes of reef fishes. BMC Evol Biol 11:338.

Seibold I, Helbig AJ. 1995. Evolutionary history of New and Old World vultures inferred from nucleotide sequences of the mitochondrial cytochrome b gene. Phil Trans R Soc Lond B Biol Sci 350:163–178.

Sekercioglu CH. 2006. Increasing awareness of avian ecological function. Trend Ecol Evol 21:464–471.

Slonaker JR. 1897. A comparative study of the area of acute vision in vertebrates. J Morph 13:445–502.

Smith HR, DeGraaf RM, Miller RS. 2002. Exhumation of food by turkey vulture. J Raptor Res 36:144–145.

Smith SA, Paselk RA. 1986. Olfactory sensitivity of the turkey vulture (*Cathartes aura*) to three carrion-associated odorants. Auk 103:586–592.

Spiegel O, Getz WM, Nathan R. 2013. Factors influencing foraging search efficiency: why do scarce lappet-faced vultures outperform ubiquitous white-backed vultures? Am Nat 181:E102–E115.

Stager KE. 1964. The role of olfaction in food location by the turkey vulture. Los Angeles County Mus Contr Sci 81:1–63.

Stevens M. 2013. Sensory ecology, behavior, and evolution. Oxford: Oxford University Press.

Stolen ED. 2000. Foraging behaviour of vultures in central Florida. Fla Field Nat 28:173–181.

Stone J. 1981. The wholemount handbook: a guide to the preparation and analysis of retinal wholemounts. Sydney: Clarendon Press.

Sun W, Li N, He S. 2002. Large-scale morphological survey of mouse retinal ganglion cells. J Comp Neurol 451:115–126.

Tabor SP, McAllister CT. 1988. Nocturnal flight by turkey vultures (*Cathartes aura*) in southcentral Texas. J Raptor Res 22:91.

Tagliarini MM, Pieczarka JC, Nagamachi CY, Rissino J, de Oliveira EHC. 2009. Chromosomal analysis in Cathartidae: distribution of heterochromatic blocks and rDNA, and phylogenetic considerations. Genetica 135:299–304.

Tucker VA. 2000. The deep fovea, sideways vision and spiral flight paths on raptors. J Exp Biol 203:3745–3754.

Ullmann JFP, Moore BA, Temple SH, Fernández-Juricic E, Collin SP. 2012. The retinal wholemount technique: a window to understanding the brain and behavior. Brain Behav Evol 79:26–44.

Veilleux CC, Lewis RJ. 2011. Effects of habitat light intensity on mammalian eye shape. Anat Rec 294:905–914.

Wallace MP, Temple SA. 1987a. Competitive interactions within and between species in a guild of avian scavengers. Auk 104:290–295.

Wallace MP, Temple SA. 1987b. Impacts of the 1982–1983 El Nino on population dynamics of Andean condors in Peru. Biotropica 20:144–150.

Walls GL. 1942. The vertebrate eye and its adaptive radiation. Bloomfield Hills: Cranbrook Institute of Science.

Walter WD, Fischer JW, Humphrey JS, Daughtery TS, Milleson MP, Tillman EA, Avery ML. 2012. Using three-dimensional flight patterns at airfields to identify hotspots for avian-aircraft collisions. Appl Geogr 35:53–59.

Wathey JC, Pettigrew JD. 1989. Quantitative analysis of the retinal ganglion cell layer and optic nerve of the barn owl *Tyto alba*. Brain Behav Evol 33:279–292.

Wilson EE, Wolkovich EM. 2011. Scavenging: how carnivores and carrion structure communities. Trend Ecol Evol 26:129–135.

Wink M. 1995. Phylogeny of Old and New world vultures (Aves: Accipitridae and Cathartidae) inferred from nucleotide sequences of the mitochondrial cytochrome b gene. Z Naturforsch 50c:868–882.

Wood CA. 1917. The fundus oculi of birds, especially as viewed by the ophthalmoscope: a study in comparative anatomy and physiology. Chicago: Lakeside Press.